Drift reinforcement design based on discontinuity network modelling

Martin Grenon & J. Hadjigeorgiou

Faculté des sciences et de génie, Département de génie des mines, de la métallurgie et des matériaux, Université Laval, Québec, Canada

Laboratoire de Mécanique des Roches
Département de génie des mines, de la métallurgie et des matériaux

ABSTRACT

The results of structural mapping are used to generate 3-D joint networks. By introducing a virtual excavation in the generated rock mass it is possible to identify all wedges that can potentially be defined at the exposed surfaces of the excavation. The number and size of these wedges are controlled by the geometry and orientation of the excavation, as well as the properties of the generated joint sets and individual random joints. Consequently it is possible to determine the stability of every individual wedge along the span of an excavation. The influence of various reinforcement strategies (type of bolts, reinforcement patterns, mesh, etc.) on the stability of an excavation is quantified. This is a prelude to an economic analysis whereby the costs associated with different stabilization techniques are assessed. This methodology is illustrated by means of three case studies in a polymetallic underground mine in the Canadian Shield.

KEYWORDS

Discontinuity network modelling; Drift stability; Cost analysis

CITATION

Grenon M, & Hadjigeorgiou J. Drift reinforcement design based on discontinuity network modelling. International Journal of Rock Mechanics and Mining Sciences (2003) 40(6), 833-845.

This is the author's version of the original manuscript. The final publication is available at Pergamon Link Online via doi:10.1016/S1365-1609(03)00044-3

1 INTRODUCTION

The primary goal of ground support in mine drifts is to protect mine workers and equipment against rock falls. Despite the development of innovative ground stabilization techniques and the increasing use of mechanized and automated equipment, rock falls remain one of the major causes of injuries and fatalities in underground metal mines. Krauland [1] has suggested that rock stabilization can be best optimized if attention is given to the economic conditions of a given site. In practice several stabilization options can meet safety requirements. From an economic viewpoint, the optimum support should result in the minimum total stabilization operation disturbance costs (Fig. 1).

Direct costs for stabilization installed at the face of an excavation include scaling, rock bolting, mesh installation, etc., while the indirect costs are stope and mine related fixed costs. Disturbance costs include complementary support (scaling, bolting, etc.) cleaning up, equipment loss, etc. The indirect costs for disturbances have to account for mine fixed costs as well as production losses. Krauland [1] makes the case that the optimal support system is one that not only meets the requirements for a safe design but also one that minimizes the economic risks associated with operational disturbances, and low direct costs.

This paper provides a methodology that can aid in the selection of a stabilization strategy while accounting for reinforcement costs. Furthermore, this paper presents a framework for quantifying the influence of different reinforcement strategies on drift stability in a Canadian hard rock mine in Northwestern Quebec. The Louvicourt Mine is a polymetallic orebody of copper, zinc, silver and gold. The mine employs transverse blasthole open stopes and paste backfill. The selected case studies are from three draw point drifts.

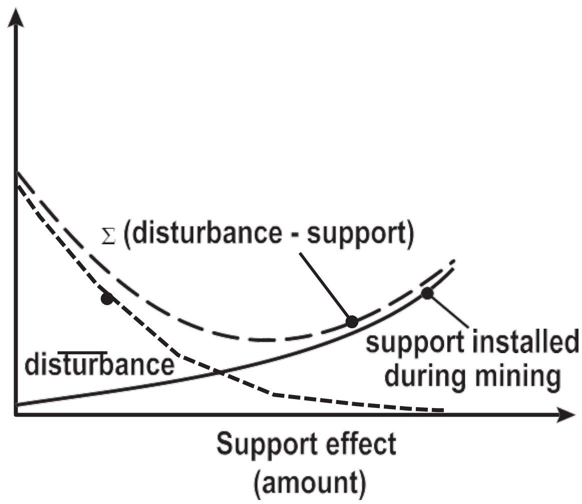

Fig. 1. The economics of stabilization, after Krauland [1].

The applied methodology relies on ground characterization to identify all structurally feasible wedges at the back of the excavations. An important element of the adopted approach is the integration in the analysis of all joints recorded during mapping. This is different from most traditional methods where only joints that are identified with a particular joint set are used in the analysis. A statistical analysis of the collected field data identifies all joint sets. Individual joints that are not associated with a particular set are defined as random. A joint network is generated using the principles of the disk model. In order to integrate the influence of random joints in the generated model it is necessary to determine their frequency and length based on the in situ data. This information is then used to generate similar random joints in the simulated rock mass. This modified procedure allows for the generation of joint sets as well as random joints. Introducing the geometry and dimensions of any excavation in generated 3-D joint network results in a realistic estimate of the number and size of wedges that can form at the sides of the excavation. Subsequent analysis determines the stability of each individual wedge, while further allowing the influence of various reinforcement strategies (bolts, reinforcement patterns, etc.). It is furthermore possible to determine the associated costs for various stabilization methods. The presented case studies investigate the efficiency of popular rock bolt types and patterns. Current work aims to validate this methodology by collecting more case studies. Once this is achieved, the proposed techniques can provide an attractive complement to traditional reinforcement design tools and can eventually be linked to more sophisticated economic models.

2 COST OF REINFORCEMENT

The choice of support systems is often influenced by previous practice, legislation, operational preferences as well as ground mechanics principles. Mechanical, resin grouted (rebar) and Swellex bolts are popular in Eastern Canadian mines [2]. These rock bolts are often used with mesh and/or shotcrete to provide the required support capacity. In practice the rock mechanics engineer has several options. If, for example, one considers that the usual bolt lengths are 1.5 and 2.1 m, placed in square or dice (star) patterns with spacing between 1, 1.2 and 1.5 m this can result in 36 different reinforcement strategies. It follows that the associated costs can influence the choice of an optimal strategy. Charette and Hadjigeorgiou [3], provide a reference for reinforcement costs (Cdn$ 1998), in Canadian mines (Fig. 2). Table 1 summarises the costs for different reinforcement options for a drift. A point of interest and concern is the range of costs, from 6.01 $/m^2$ for 1.5 m long mechanical bolts in a square pattern of 1.5 x 1.5 m^2 to 52.50 $/m^2$ for 2.1 m long rebars installed in a star tight pattern of 1.0 x 1.0 m2. The economic consequences of selecting any one option become apparent when these costs are extrapolated for the total number of drifts in a mine.

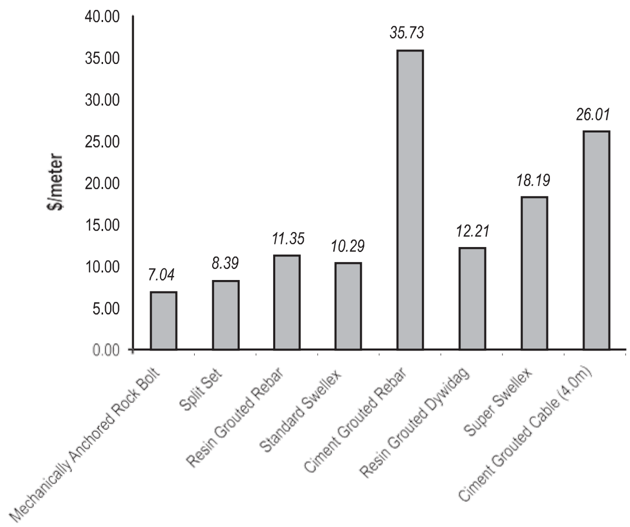

Fig. 2. Reinforcement costs per meter of bolt, after Charette and Hadjigeorgiou [3].

Table 1. Costs associated with various bolts types under different patterns

Reinforcement specifications			Mechanical ($/m^2)	Rebar ($/m^2)	Swellex ($/m^2)
Pattern	Spacing (m^2)	Length (m)			
Square	1.0 X1.0	1.5	12.53	20.19	18.31
Square	1.2 X1.2	1.5	8.98	14.47	13.12
Square	1.5 X1.5	1.5	6.01	9.69	8.79
Square	1.0 X1.0	2.1	17.54	28.27	25.63
Square	1.2 X1.2	2.1	12.57	20.26	18.37
Square	1.5 X1.5	2.1	8.42	13.57	12.31
Star	1.0 X 1.0	1.5	23.26	37.50	34.00
Star	1.2 X 1.2	1.5	16.31	26.29	23.84
Star	1.5 X 1.5	1.5	10.71	17.26	15.65
Star	1.0 X 1.0	2.1	32.57	52.50	47.60
Star	1.2 X 1.2	2.1	22.83	36.81	33.37
Star	1.5 X 1.5	2.1	14.99	24.17	21.91

3 QUANTIFYING THE PROBABILITY OF INSTABILITY

Using the results of structural mapping, a 3-D joint network is constructed for the investigated rock mass zone using a 3-D joint generation software package, Stereoblock. The details of the model are described in [4]. The essential premise is the applicability of the Poisson disk model proposed by Baecher et al. [5].

Fig. 3 provides an overview of the applied methodology. Scanline surveys are used to determine joint set orientation, spacing and trace length distributions. To minimize the in situ sampling bias, at least three different scanline orientations are used in the field. Stereoblock uses this information to generate 3-D joint networks for a given rock volume. Once a 3-D joint network is constructed, it is possible to generate a series of scanlines randomly oriented in space. This results in sampling of the generated rock mass. The use of random scanlines minimizes orientation bias. This process allows the virtual mapping of the generated 3-D jointed rock mass. It is hence possible to characterize the generated rock mass and produce a stereographic representation of the joints, as well as spacing and trace length distributions. The procedure is completed when the field input data are compared with the information resulting from the simulated 3-D rock mass using a χ^2 analysis. This somewhat crude validation exercise is considered acceptable for the given application.

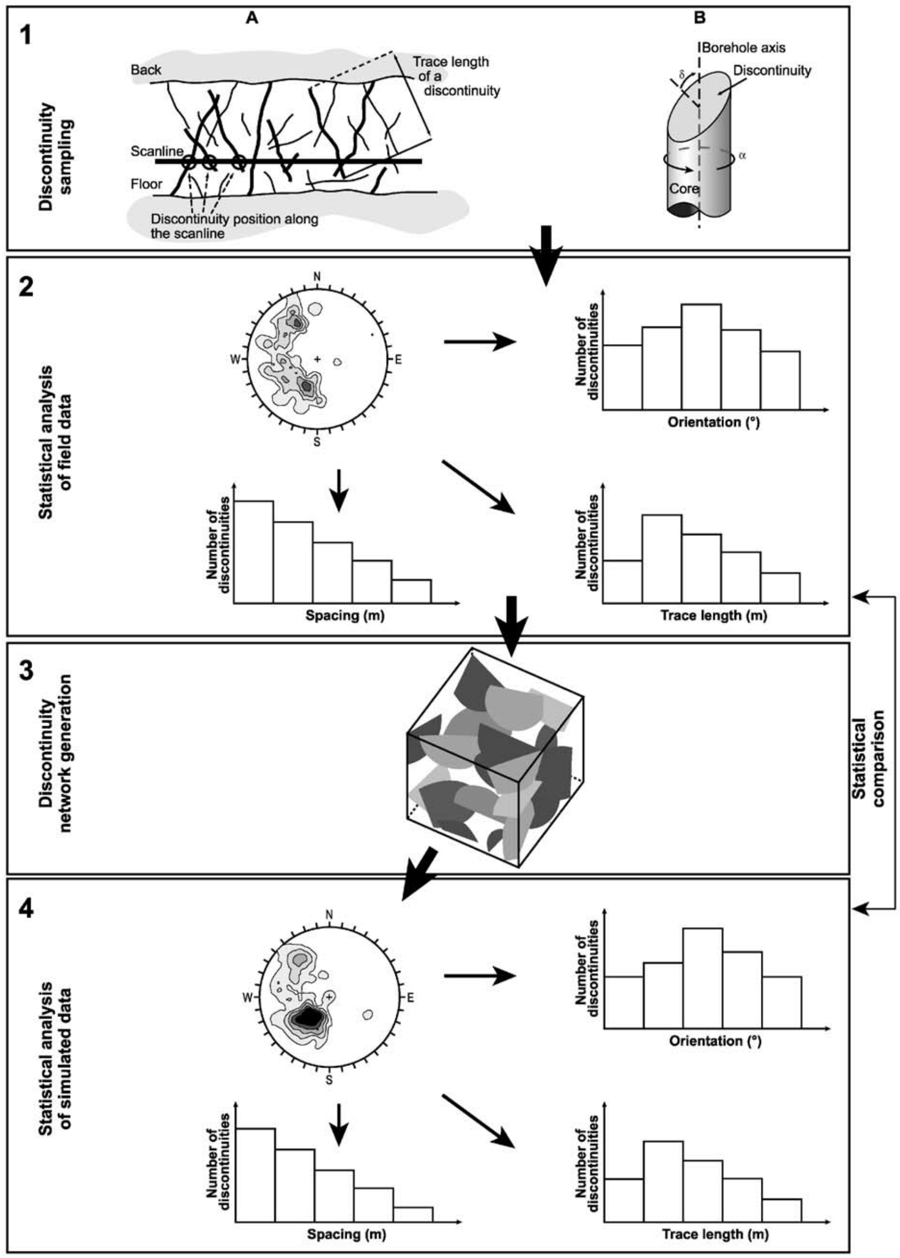

Fig. 3. The stereoblock methodology.

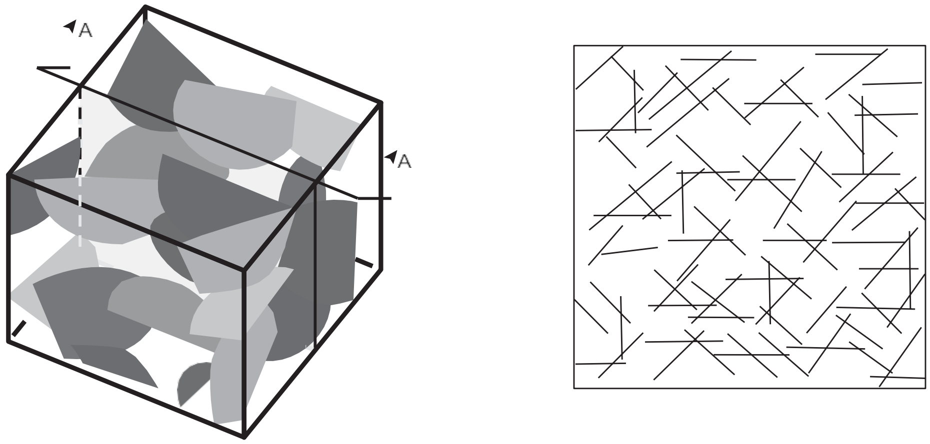

Fig. 4. Section cut through the simulated joint network.

Once a realistic 3-D representation has been constructed and validated, it is then possible to introduce any form, size and shape of excavation. If the mapping has revealed the presence of a large-scale discrete structural feature, such as a fault, this can also be introduced in the generated jointed rock mass. The mechanical properties of the discontinuities were defined by the Mohr–Coulomb criterion, allowing for variations in the input data. Once the excavation is introduced in the generated rock mass, a number of discontinuities intersect the back and sides of the excavation. A conceptual representation is provided in Fig. 4. Furthermore, as discontinuities intersect each other they can define discrete blocks in the excavation. Naturally the form of any such defined blocks has an obvious impact on the stability of the excavation. It is the authors' field experience that tetrahedral blocks are the most common type. This is in agreement with observations by Windsor [6], Kuszmaul [7] and Mauldon [8]. As a result the present analysis focuses in identifying all possible tetrahedral blocks at any face of an excavation (Fig. 5).

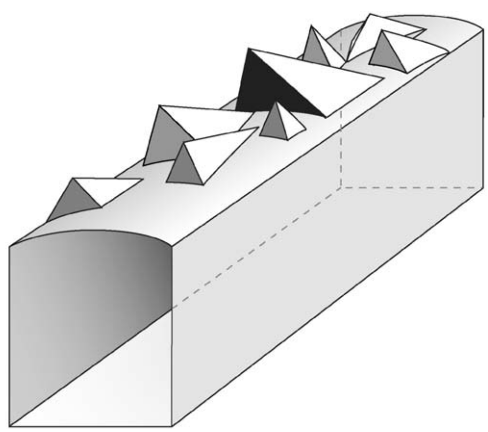

Fig. 5. Schematic of rock blocks potentially formed at the back of a drift.

Tetrahedral blocks are defined by their base area, apex length and volume. Subsequently, all resulting distributions, for every block property are calculated. Furthermore, each discontinuity that contributes to the creation of a wedge is tracked, thus enabling the determination of the most critical joint sets for a given drift geometry and orientation.

In order to assess the global stability of a drift, the individual stability of every tetrahedral wedge at the face of the excavation is determined. It is then possible to determine the associated probability of failure for any given drift size and orientation.

The limit equilibrium method is used to determine the stability of every individual block, after Hoek and Brown [9] and the influence of reinforcement, after Li [10]. The factor of safety is defined as

(a) gravity driven (falling)

$$FS = \frac{\sum_{l=1}^{n} T_g^l}{W_g} \quad (1)$$

(b) Sliding along a single plane

$$FS = \frac{N_i \tan\phi_i + A_i c_i}{S_i} + \frac{\sum_{l=1}^{n}\left[T_{ni}^l \tan\phi_i + T_{si}^l\right]}{S_i} \quad (2)$$

(c) Wedge sliding along the line of intersection of two planes

$$FS = \frac{N_i \tan\phi_i + N_j \tan\phi_j + A_i c_i + A_j c_j}{S_{ij}} + \frac{\sum_{l=1}^{n}\left[T_{ni}^l \tan\phi_i + T_{nj}^l \tan\phi_j + T_{sij}^l\right]}{S_{ij}} \quad (3)$$

where n is the number of bolts, W_g is the weight in the direction of the gravity, N_i is the component of the block's weight normal to plane (i) multiplied by the area of plane (A_i), S_i is the component of the block's weight tangential to plane (i) in the direction of sliding, S_{ij} is the component of the block's weight in the direction of the intersection line between plane i and j; T_g is the component of the bolt capacity (T) in the gravity direction, T_{ni} is the component of the bolt capacity (T) normal to plane (i), T_{si} is the component of the bolt capacity (T) tangential to plane (i) and in the sliding direction, T_{sij} is the component of the bolt capacity (T) in the direction of the line of intersection of plane i and j; Ai is the area of plane (i), c_i is the cohesion of plane (i), and ϕ_i is the friction angle of plane (i).

The above approach can account for several discontinuity sets, random joints as well as the finite dimension of discontinuities and the mechanical properties of the rock mass.

4 CASE STUDIES

Structural scanline mapping campaigns were undertaken at an underground mine site in northeastern Canada. The Louvicourt mine, is a polymetallic orebody of copper, zinc, silver and gold. This volcanogenic massive sulfide deposit lies at a depth of 475 m from the surface, and is part of the Abitibi Greenstone belt within the Precambrian shield of Eastern Canada. The mine uses transverse blasthole open stopes, 50 m in length, 15 m in width and 30 m in height. The operation uses paste backfill.

Scanline mapping was used to record orientation, position and trace length of discontinuities. Following a visual identification of the dominant discontinuity sets (Fig. 6), their mean orientation and coefficient of dispersion (K) were determined based on Fisher [11]. Mean normal spacing, mean trace length and standard deviation were evaluated for every discontinuity set (Tables 2–4). Site #1 is characterized by the presence of four discontinuity sets, while sites #2 and #3 are characterized by two sets. It was noted that random joints, (i.e. those that are not associated with any sets) represent around 30% all discontinuities for the three sites. Consequently, in an effort to quantify their influence, the total spacing and the mean trace length of all random discontinuities were evaluated. Corrections for joint censoring were not undertaken at these sites, as more then 98% of the joints had a length inferior to the sampling window (3.5 m) and both extremities were visible.

Based on these preliminary data analysis, a 3-D discontinuity network was generated for each site. The generation volume was 10 m x 10 m x 70 m and oriented north. The structural properties of the generated discontinuity sets were compared to the in situ ones. Fisher univariate distributions were used to describe discontinuity dispersion around the mean value. Exponential distributions were used to characterize the discontinuity spacing, while lognormal distributions were used to define trace lengths. The detailed results are presented in Tables 5–7, where 27 out of 30 distributions were declared statistically similar and the simulations were considered acceptable.

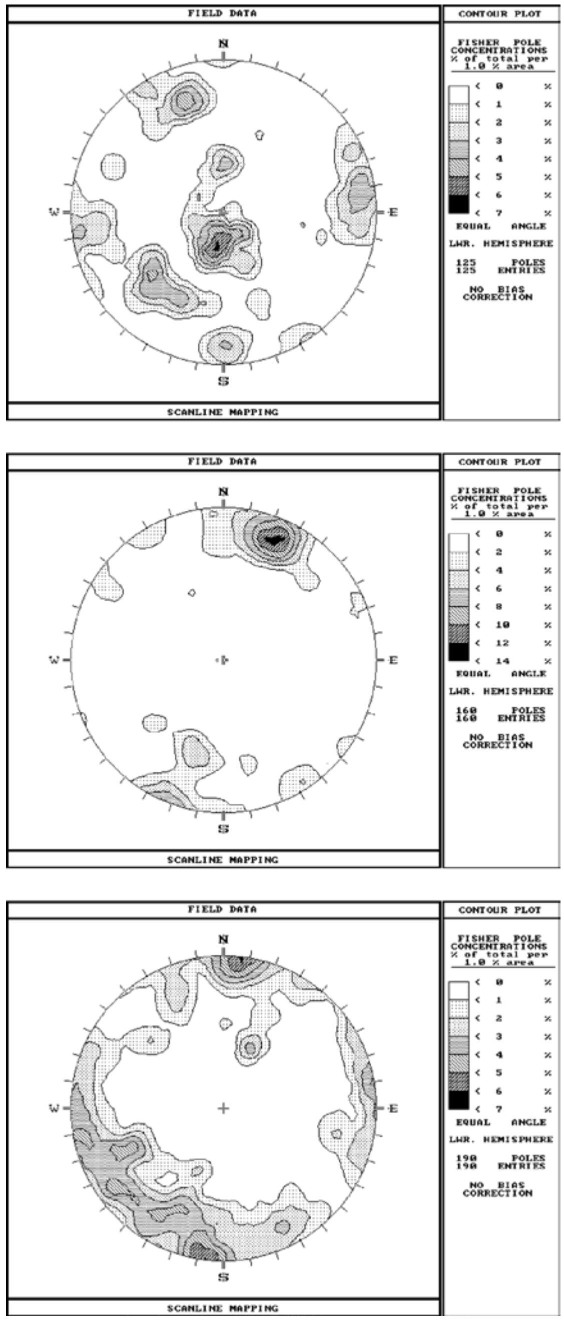

Fig. 6. Stereonet for sites #1, #2 and #3.

Based on a limited number of direct shear tests and assuming normal distributions, the angle of friction was determined as $30 \pm 2.5°$ with a cohesion value of 300 ± 50 kN. Subsequently, for all generated discontinuities, the mechanical properties of the discontinuities were randomly selected from these distributions. It is felt that this approach is justified based on the engineering constraints of the analysis.

The individual stability of every wedge that formed at back of the three 4.4 m x 6m x 60 m drifts was determined. All three drifts were oriented north and horizontal. The drifts were supported by 2.1 m grouted rebar bolts on a 1.2 x 1.2 m^2 pattern and a Gage 9 welded mesh. In the stability analysis mesh capacity was calculated based on the work of Tannant [12], whereby a Gage 9 mesh, used with a 1.2 x 1.2 m^2 bolt pattern, can sustain blocks of up to 1.5 ton.

Table 2. Statistical analysis of the first mapped discontinuity network

	Orientation (º)	*K*	Average trace length (m)	Trace length standard dev. (m)	Normal spacing (m)
Set 1	22/238	26	1.20	1.20	0.34
Set 2	64/009	29	1.00	0.90	0.43
Set 3	76/128	47	1.50	1.20	1.20
Set 4	90/234	26	1.50	1.50	0.56
Random	—	—	1.70	2.00	0.63

Table 3. Statistical analysis of the second mapped discontinuity network

	Orientation (º)	*K*	Average trace length (m)	Trace length standard dev. (m)	Normal spacing (m)
Set 1	85/202	60	1.60	1.20	0.45
Set 2	61/037	13	1.40	1.30	0.70
Random	—	—	1.10	1.00	0.37

Table 4. Statistical analysis of the third mapped discontinuity network

	Orientation (º)	*K*	Average trace length (m)	Trace length standard dev. (m)	Normal spacing (m)
Set 1	89/188	77	1.07	0.62	0.39
Set 2	75/036	36	1.21	0.66	0.36
Random	—	—	1.36	0.93	0.37

Table 5. Validation of the simulated network for site #1

	Parameter	Distribution	Number of classes	χ^2 test	Accepted
Set 1	Orientation	Fisher univariate	6	6.01	Yes
	Spacing	Exponential negative	5	2.16	Yes
	Trace	Lognormal	8	8.77	Yes
Set 2	Orientation	Fisher univariate	6	10.61	Yes
	Spacing	Exponential negative	5	3.45	Yes
	Trace	Lognormal	7	6.36	Yes
Set 3	Orientation	Fisher univariate	5	1.35	Yes
	Spacing	Exponential negative	6	3.37	Yes
	Trace	Lognormal	6	10.72	Yes
Set 4	Orientation	Fisher univariate	7	4.69	Yes
	Spacing	Exponential negative	7	8.18	Yes
	Trace	Lognormal	6	31.15	No
Random	Spacing	Exponential negative	8	18.87	No
	Trace	Lognormal	5	6.88	Yes

Table 6. Validation of the simulated network for site #2

	Parameter	Distribution	Number of classes	χ^2 test	Accepted
Set 1	Orientation	Fisher univariate	6	4.39	Yes
	Spacing	Exponential negative	5	7.49	Yes
	Trace	Lognormal	7	8.05	Yes
Set 2	Orientation	Fisher univariate	8	2.77	Yes
	Spacing	Exponential negative	5	2.17	Yes
	Trace	Lognormal	8	13.15	Yes
Random	Spacing	Exponential negative	5	1.72	Yes
	Trace	Lognormal	8	26.35	No

Table 7. Validation of the simulated network for site #3

	Parameter	Distribution	Number of classes	χ^2 test	Accepted
Set 1	Orientation	Fisher univariate	8	3.71	Yes
	Spacing	Exponential negative	7	3.70	Yes
	Trace	Lognormal	8	5.09	Yes
Set 2	Orientation	Fisher univariate	6	1.74	Yes
	Spacing	Exponential negative	8	3.56	Yes
	Trace	Lognormal	8	46.29	No
Random	Spacing	Exponential negative	6	2.30	Yes
	Trace	Lognormal	6	6.41	Yes

5 STABILITY AND COST ANALYSIS

The geometric properties of all blocks intersecting the drift back for site #1 are presented in Fig. 7. A total of 479 blocks were created at the back of the simulated drift with the majority of blocks being relatively small in size. In fact, 2% of the blocks have an apex length exceeding 2.1 m and no block has a volume greater than 0.5 m^3. The influence of random discontinuities is illustrated in Fig. 7d, where more than 32% of the created blocks are formed with at least 1 random discontinuity (joint set 0).

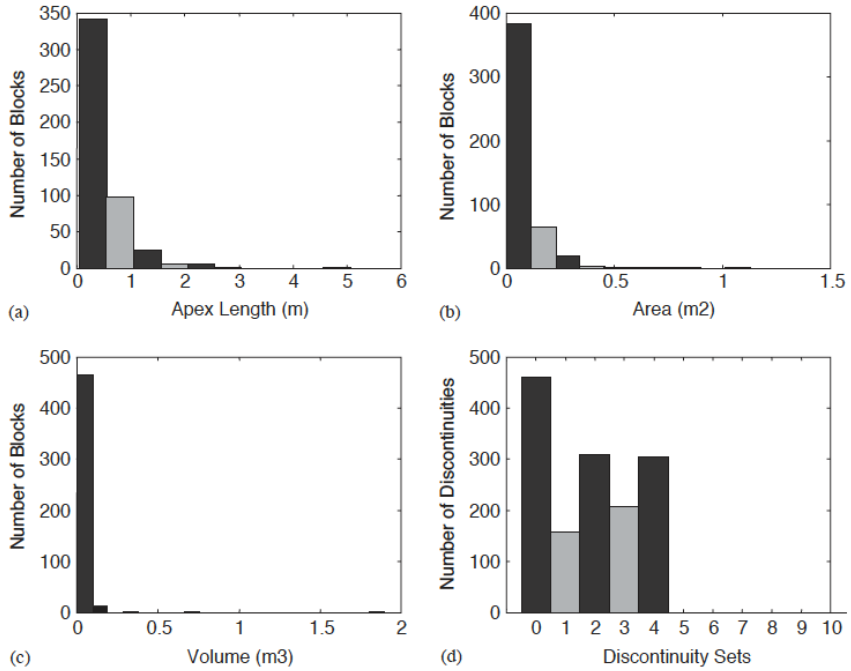

Fig. 7. Quantification of the geometric distributions for site #1: (a) number of blocks versus apex length; (b) number of blocks versus base area; (c) number of blocks versus volume; and (d) number of discontinuities per set (NB: Set 0 stands for random joints).

Fig. 8 shows the distribution of safety factors for each block. A first attempt to evaluate the efficiency of the reinforcement system relied on determining the resulting factor of safety for every block (Fig. 8b). It is of interest to note the two extremes in the histogram. A number of blocks stabilized with reinforcement have a high factor of safety. These blocks were identified as the larger blocks generated in the rock mass, with their length and area distributions plotted in Figs. 8c and d. Rock bolts are more than adequate in supporting the larger blocks on the drift back. At first glance, the number of unstable blocks (88% of the generated blocks) is somewhat alarming. A closer inspection reveals that these blocks are very small in size, thus posing no immediate concern. In practice smaller blocks are likely to fall during blasting and scaling. Installation of mesh (Gage 9) can retain such small blocks. Based on the undertaken stability the mesh could retain 99% of blocks not directly reinforced by rock bolts. It follows that the employed combination of rebar and weld mesh provided the required support for the back of the drift.

A common design concern is the adequacy of the reinforcement pattern and bolt length. The performance of the standard mine reinforcement pattern was evaluated once it was introduced in the generated 3-D joint rock mass. It was shown that the length of the rebar bolts was longer that the block apex length in 98% of the generated blocks. Fig. 8e shows the number of bolts that intercept a rock block defined by the discontinuities in the back of the drift. The results indicate that, out of the 306 rock bolts installed, 43 intercepted a block. In this case 436 blocks were not intercepted by any rock bolts.

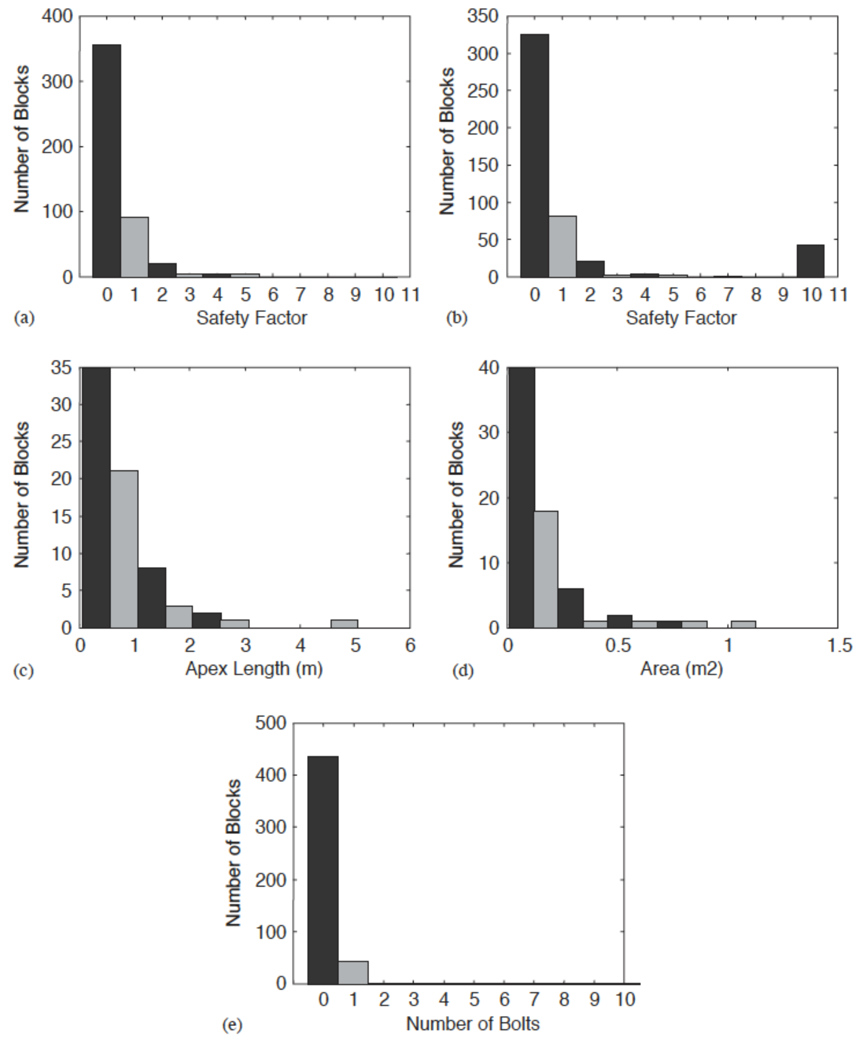

Fig. 8. Stability information for site #1: (a) safety factor distribution (without reinforcement); (b) safety factor distribution (with reinforcement); (c) number of reinforced rock blocks versus apex length; (d) number of reinforced rock blocks versus area; and (e) number of blocks intercepted by a bolt.

Figs. 9a–c present the results of site #2 where 297 small blocks were created at the back of the drift. Random discontinuities were critical in the formation of rock blocks (Fig. 9d). Safety factor distributions for the case of no reinforcement, is presented in Fig. 10a, where a total of 13% of the blocks are characterized by a safety factor greater than 1. When reinforcement is used, 17% of the blocks are adequately stabilized (Fig. 10b). The analysis indicates that all created blocks are stable, when a combination of rebar and weld mesh, is used to stabilize the back of the drift.

Fig. 11 presents the results for drift #3 where 621 blocks were created along the back of the drift. These blocks are small in size (Fig. 11a–c). The introduction of random discontinuities is critical for the subsequent stability analysis. Random discontinuities are responsible for the formation of the majority of generated rock blocks. The safety factor distribution is presented in Fig. 12a, for the case where no reinforcement is applied. Under these conditions only of 15% of the blocks are characterized by a safety factor greater than 1. The use of rock bolt reinforcement results in adequately stabilizing 19% of the generated blocks (Fig. 12b). If the support system, however, includes the application of mesh the back of the excavation, all generated blocks are stabilised.

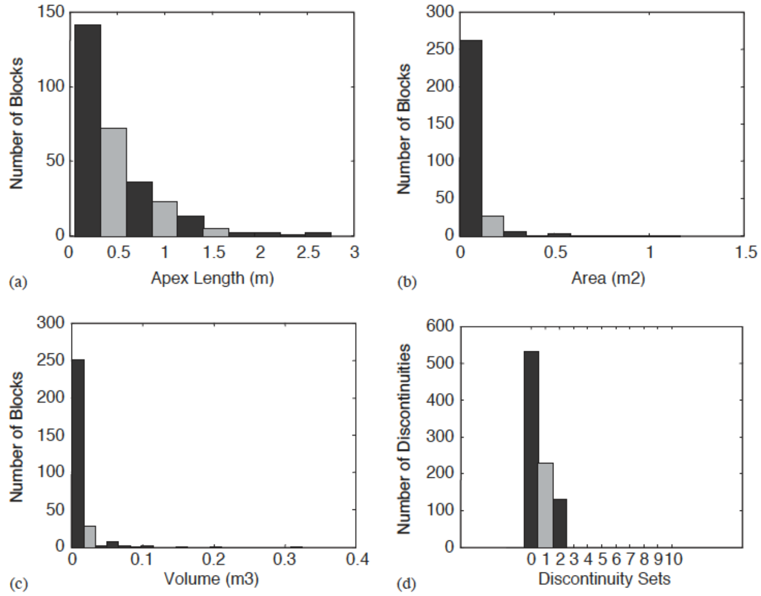

Fig. 9. Quantification of the geometric distributions for site #2: (a) number of blocks versus apex length; (b) number of blocks versus base area; (c) number of blocks versus volume; and (d) number of discontinuities per set.

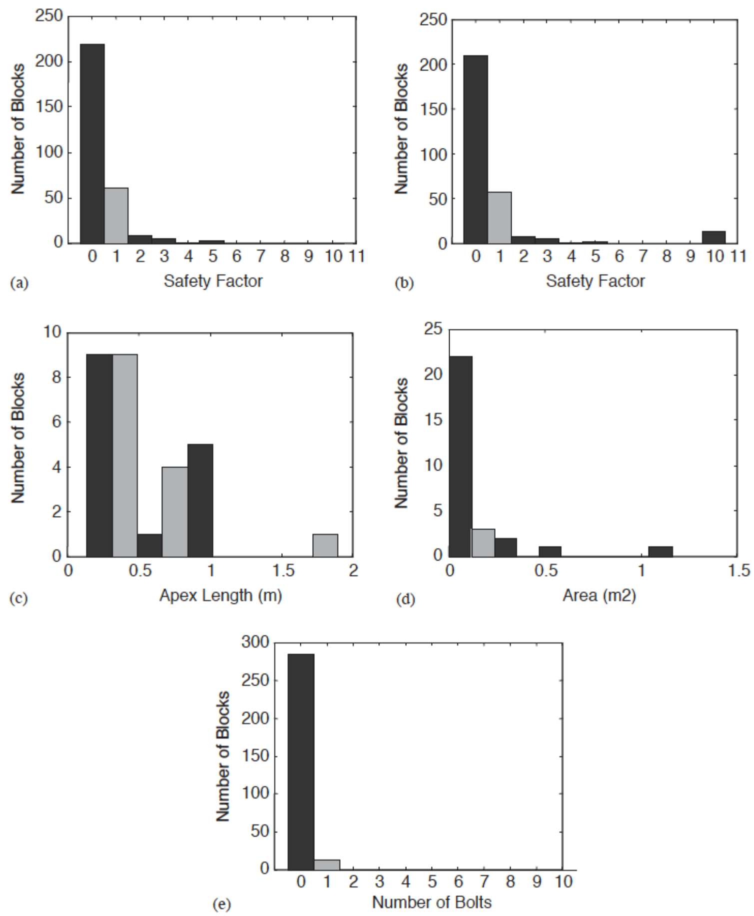

Fig. 10. Stability information for site #2: (a) safety factor distribution (without reinforcement); (b) safety factor distribution (with reinforcement); (c) number of reinforced rock blocks versus apex

length; (d) number of reinforced rock blocks versus area; and (e) number of blocks intercepted by a bolt.

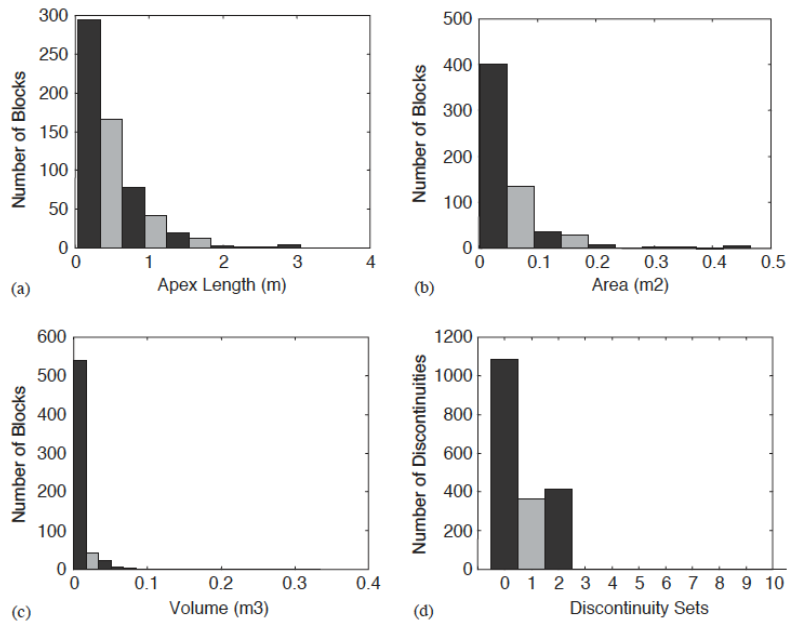

Fig. 11. Quantification of the geometric distributions for site #3: (a) number of blocks versus apex length; (b) number of blocks versus base area; (c) number of blocks versus volume; and (d) number of discontinuities per set.

Table 8. Number of stable blocks (%) at the back of the drift

Layout pattern (m^2)	Mechanical, 1.5 m	Rebar, 1.5 m	Swellex, 1.5 m	Mechanical, 2.1 m	Rebar, 2.1 m	Swellex, 2.1 m
Square, 1.0 X 1.0	25	25	25	25	25	25
Star, 1.0 X 1.0	35	35	35	35	35	35
Square, 1.2 X 1.2	20	22	22	20	20	22
Star, 1.2 X 1.2	26	26	26	26	26	26
Square, 1.5 X 1.5	18	18	18	18	18	18
Star, 1.5 X 1.5	22	22	22	22	22	22

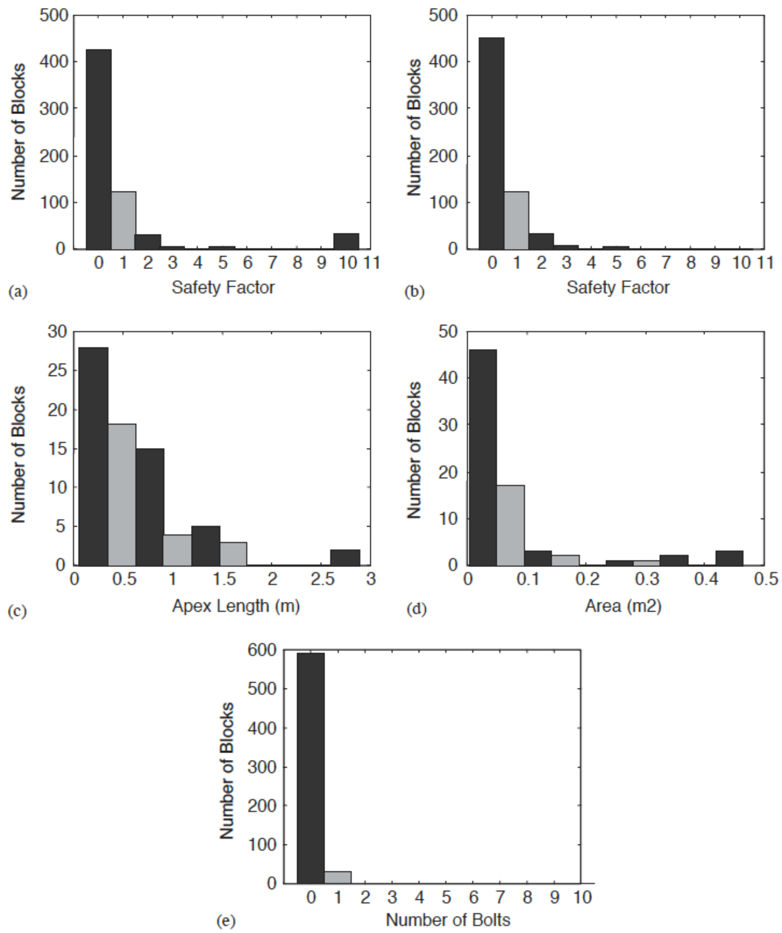

Fig. 12. Stability information for site #3: (a) safety factor distribution (without reinforcement); (b) safety factor distribution (with reinforcement); (c) number of reinforced rock blocks versus apex length; (d) number of reinforced rock blocks versus area; and (e) number of blocks intercepted by a bolt.

Further simulations were performed to investigate the use of other reinforcement systems. Table 8 presents the percentage of stable blocks for the various reinforcement options considered at site #1. For the studied rock mass it was shown that increasing the bolt length from 1.5 or 2.1 m did not result in an important increase on the number of intersected reinforced rock blocks. In this case all bolting configurations were acceptable. As discussed earlier, the choice for a particular bolt type may be due to a variety of technical reasons: ground susceptible to rock bursting, corrosion, presence of water, etc. Tightening the reinforcement pattern, from 1.5 x 1.5 m^2 to 1.0 x 1.0 m^2, resulted in increased excavation stability. This is quantified by the number of stable blocks (Table 8).

The real interest in this approach lies in comparing the cost and efficiency of different reinforcement strategies. Assuming that the cause of instability is wedge failure it was shown in Tables 1 and 8 that several reinforcement options are available. Equivalent stabilization systems, however, can have considerably different rock bolting costs. For example, mechanical rock bolts in a square pattern of 1.0 x 1.0 m^2 offer the same acceptable degree of stability to a dice pattern of 1.2 x 1.2 m^2. The cost associated with the first pattern is 77% of the second one. If the length of the bolts is allowed to vary, the cost of the square pattern 1.0 x 1.0 m^2 with a bolt length of 1.5 m is only 55% of the cost of the 1.2 x 1.2 m^2 using 2.1 m long mechanical bolts.

The above analysis does not address quality control issues, long-term performance of the different options, stand-up time after the excavation is opened, ravelling effects and the influence of local stress fields. For example it is recognised that when a permanent drift is located near a blasting area resin-grouted or Swellex bolts are more appropriate than mechanical bolts. It can be argued that the installation of 1.5 m long Swellex bolts, over a pattern of 1.5 x 1.5 m^2, offers the same level of stability as 2.1 m resin grouted rebar bolts over a dice pattern of 1.2 x 1.2 m^2. The cost of the first option is half the cost of the second one. On a yearly basis at a mine site, these differences may lead to substantial reduction in costs.

6 CONCLUSIONS

This paper reports on the use of an engineering methodology to generate a 3-D representation of discontinuity networks based on structural field data. Scanline surveys are used to determine joint set orientation, spacing and trace length distributions and to generate 3-D joint networks. Following a validation process whereby field input data are compared with the structural data resulting from the simulated 3-D network it is then possible to introduce any form, size and shape of excavation in the simulated rock mass.

A number of discontinuities intersecting the back and sides of the excavation define discrete blocks which are analysed using limit equilibrium techniques.

Three case studies were used to evaluate the stability of all possible wedges formed around the back of drifts at the Louvicourt Mine. It was then possible to determine the stability of individual wedges along the length of the excavations. The influence of different stabilization strategies on the stability of the excavations was quantified by means of safety factor distributions. Consequently tests were undertaken to assure that the length of the reinforcement units was adequate and the mesh would capture smaller blocks between bolts. The undertaken analysis however does not account for other factors that may influence the choice of strategies. These may include quality control, long-term performance, etc.

Once equivalent stabilizations measures are identified it is possible to attach monetary costs and identify the more attractive options. These decisions have important consequences on the profitability of mining operations.

ACKNOWLEDGEMENTS

The financial support of the National Science and Engineering Council of Canada and the Institut de Recherche en Santé et Sécurité au Travail du Quebec is greatly appreciated. The authors further acknowledge the cooperation of the Louvicourt Mine.

REFERENCES

[1] Krauland N. Rock bolting, economy. Proceedings of the International Symposium on Rock Bolting, Abisko. 1983. p. 499–507.

[2] Lemy F, Hadjigeorgiou J, Charette F. E! tat actuel de l’utilisation du boulonnage dans les mines souterraines en roche dure du Québec. Can Tunnelling 1998;97–106.

[3] Charette F, Hadjigeorgiou J. Guide pratique du soutènement minier. Québec: Association minière du, 1999. p. 117.

[4] Grenon M. Conception des excavations souterraines à l’aide de la modélisation des réseaux de discontinuités. Ph.D. thèses, Université! Laval, 2000.

[5] Baecher GB, Lanney NA, Einstein HH. Statistical description of rock properties, sampling. Proceedings of the 18th US Symposium on Rock Mechanics, Colorado, 1977. p. 5C1.1–5C1.8.

[6] Windsor CR, Keynote lecture: systematic design of reinforcement and support schemes for excavations in jointed rock. Proceedings of the International Symposium on Ground Support, Kargoorlie, Australia. Balkema: Rotterdam, 1999. p. 35–58.
[7] Kuszmaul JS. Estimating keyblock sizes in underground excavations: accounting for joint set spacing. Int J Rock Mech Min Sci & Geomech Abstr 1999;36:217–32.
[8] Mauldon M. Keyblock probabilities and size distributions: a first model for impesistent 2-D fractures. Int J Rock Mech Min Sci & Geomech Abstr 1995;32:575–83.
[9] Hoek E, Brown ET. Underground excavations in rock. London: The Institution of Mining and Metallurgy, 1980.
[10] Li B. The stability of wedges formed by three intersecting discontinuities in the rock surrounding underground excavations. Ph.D. thesis, University of Toronto, 1991.
[11] Fisher R. Dispersion on a sphere. Proceedings of the Royal Society of London 1953;A217:295–305.
[12] Tannant D. Load capacity, stiffness of welded-wire mesh. Proceedings of the 48th Canadian Geotechnical Conference, Vancouver, Canada, 1995.